Report on

# Bow Shock Formation in a Supersonic Flow over a Wedge

Case Study Project

Under the guidance of
**Prof. Shivasubramanian Gopalakrishnan**

Submitted by
**Ashley Melvin**

# ACKNOWLEDGEMENT

I would like to express my sincere thanks to **Prof. Shivasubramanian Gopalakrishnan** for his supervision, valued suggestions and timely advices. I am extremely grateful for his patient efforts in making me understand the required concepts and principles behind this work. I would also like to thank all my friends and my parents for their continued support and encouragement, without which the report could not have been completed. I would also like to thank each and everyone who have knowingly or unknowingly helped me in completing this work.

# Contents

1. Introduction 1

2. Governing Equations 1

2.1. Stand-off Distance 2

2.1.1. The Time-dependent Technique: Application to Bow Shocks 3

3. Implementation in OpenFOAM 4

3.1. Problem Statement 4

3.2. Geometry & Meshing 4

3.3. Initial & Boundary Conditions 5

3.4. Solver 6

4. Results 6

5. Conclusion 9

References 10

# 1. Introduction

A careful observation of the oblique shock relation shows that for every Mach number, there is a maximum angle of deflection. For example, the oblique shock $\theta - \beta - M$ relation (fig.1) shows that for $M = 1.5$, the maximum deflection angle $\theta_{max}$ is $12^o$. So what happens to $M = 1.5$ flow deflected at an angle more than $12^o$?

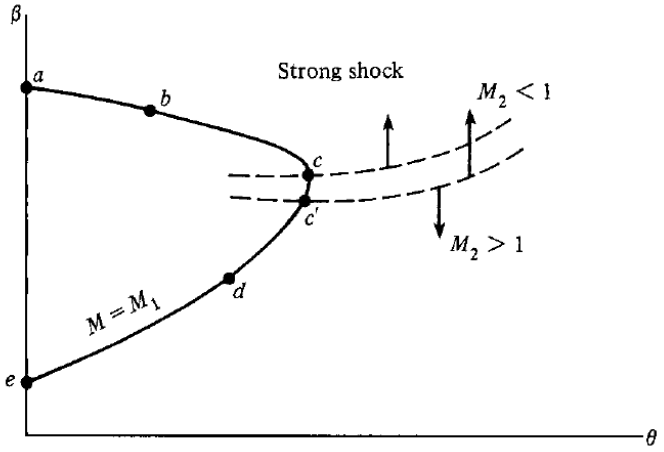


Figure 1. $\theta - \beta - M$ diagram for $M = M_1$ [1].

When a flow of given Mach number encounters a body which forces the flow to deviate more than the achievable deflection angle for an attached oblique shock, the oblique shock transforms into a curved detached shock. These curved detached shocks are also called bow shocks. Since the deflection angle required for the formation of bow shocks is high, they are often seen forming around blunt bodies. The bow shock significantly increases the drag in a body. This property is used in the design of return capsules during space mission to slow down the vehicle during atmospheric re-entry.

# 2. Governing Equations

The Navier-Stokes equations for an inviscid, compressible flow in an arbitrary domain is

$$\frac{\partial(\rho\vec{u})}{\partial t} + \nabla.[\vec{u}(\rho\vec{u})] + \nabla p = 0$$

where all symbols have their usual meaning. The Navier-Stokes equation is supplemented with the conservation of mass

$$\frac{\partial \rho}{\partial t} + \nabla.(\rho\vec{u}) = 0$$

Conservation of total energy for an inviscid compressible flow gives

$$\frac{\partial(\rho E)}{\partial t} + \nabla.[\vec{u}(\rho E)] + \nabla.(p\vec{u}) = 0$$

where the total energy density $E = e + |\vec{u}|/2$ with $e$ the specific internal energy.

The 3 equations are supplemented with an equation of state which is the isentropic relation

$$\frac{dp}{d\rho} = \left(\frac{\partial p}{\partial \rho}\right)_s = a^2$$

where $a$ is the speed of sound.

## 2.1. Stand-off Distance

Consider a supersonic flow over a blunt body as shown in fig. 2. Here the shock wave stands at a distance $\delta$ from the nose of the body. This distance is defined as stand-off distance or shock detachment distance. At point $a$, the shock wave is normal to the flow and acts as a normal shock wave. At points $b$ and $c$, the shock wave is much weaker and acts like an oblique shock wave. The shock gets weaker away from the body, eventually evolving into Mach waves at large distances from the body.

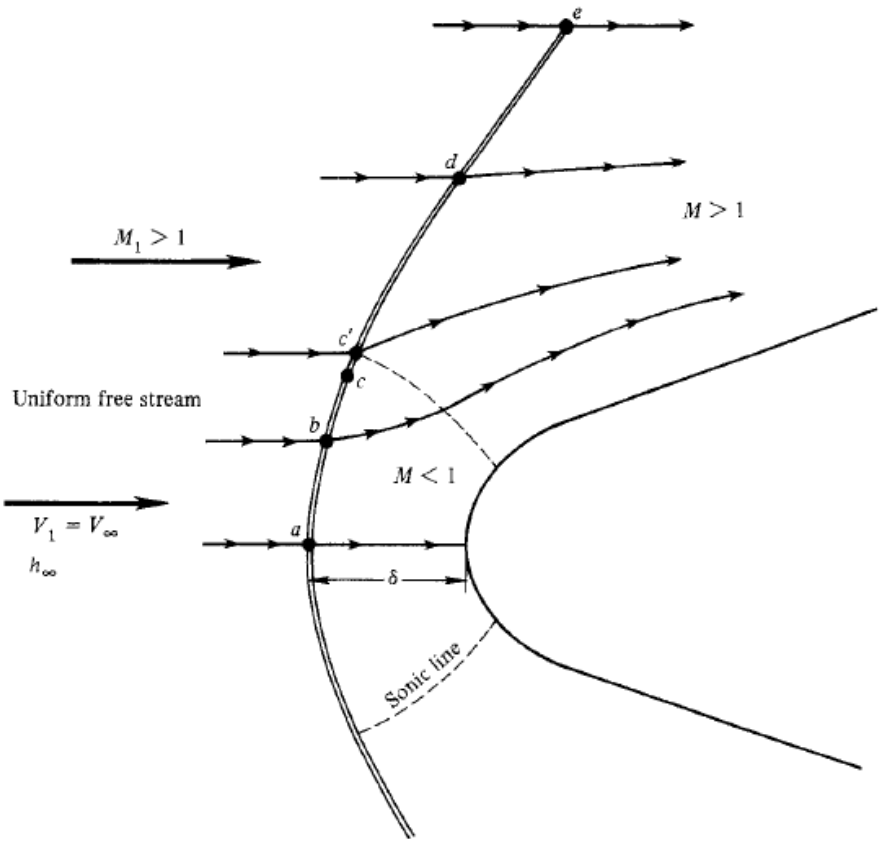


Figure 2. Supersonic flow over a blunt body [2].

The shape of the shock wave, stand-off distance $\delta$, and the flow field between shock and the body depend on the free stream Mach number $M_1$ and the shape and size of the blunt body. Unlike normal and oblique shock waves, solution to bow shock waves cannot be theoretically predicted [3].

## 2.1.1. The Time-dependent Technique: Application to Bow Shocks

Consider a supersonic flow over a blunt body as shown in fig .3. The shape of the body is given by $b = b(y)$. For a given free stream Mach number, the shape and the position of the body, shock wave is to be calculated.

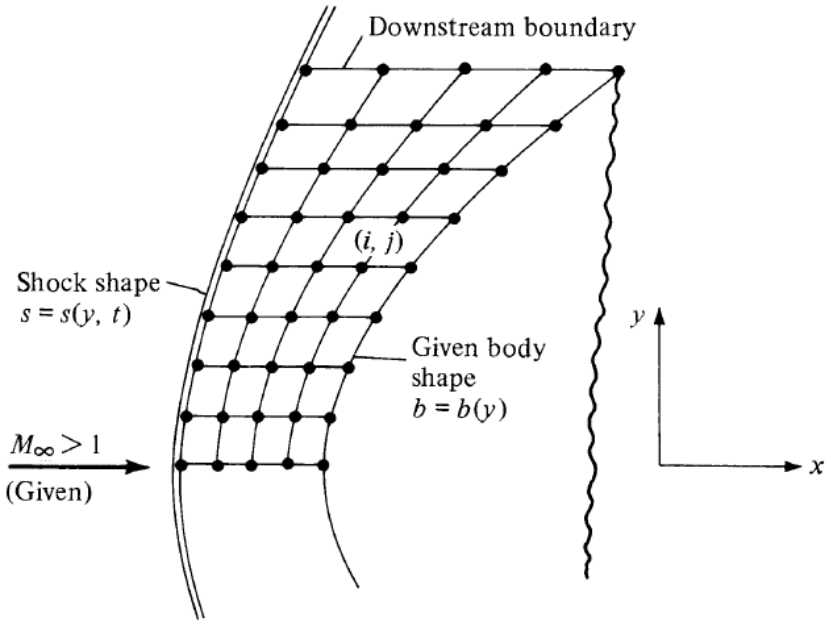


Figure 3. Blunt-body supersonic flow field in physical plane [2].

The governing equations for the flow is described in section 2.

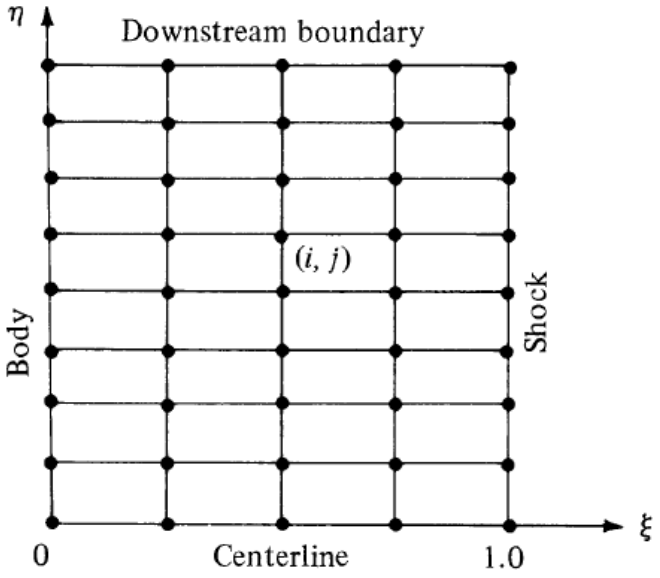


Figure 4. Blunt-body supersonic flow field in computational plane [2].

For the ease of calculation, application of finite differences in a rectangular grid is preferred. Consider the transformation

$$\xi = \frac{x - b}{s - b} \quad \text{and} \quad \eta = y$$

where $b = b(y)$ gives the abscissa of the body and $s = s(y, t)$ gives the abscissa of the shock. The above transformation produces a rectangular grid in the computational plane as shown in fig. 4.

The solution to the flow is calculated by assuming a shock (position and shape) initially. With the assumed shock, the appropriate boundary (far-field and body surface) and jump (shock) conditions are applied. The governing equations are solved using an appropriate scheme. The predictor-corrector method, like MacCormack's technique, is used to converge the solution to steady state as shown in fig. 5.

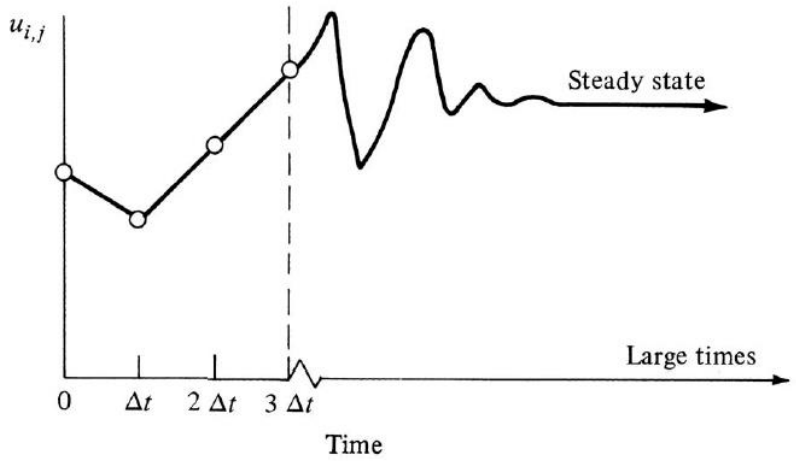


Figure 5. Typical variation of a flow field variable with time/iteration [2].

# 3. Implementation in OpenFOAM

## 3.1. Problem Statement

The problem considers a supersonic flow of air at $M = 1.5$ over a wedge of angle $23^o$. The free stream pressure and temperature is 81135 Pa and 145.768 K respectively.

## 3.2. Geometry & Meshing

The geometry of the wedge is shown in fig. 6. The dimensions are as mentioned in fig. 6. The wedge angle is $23^o$. The depth (into the sheet) of the geometry is 1 cm. The geometry was created using blockMesh utility. The meshing is simpleGrading.

The geometry is divided into 3 blocks. Each block is meshed separately, with blocks 1 and 2 being more refined than block 3. The cells are inflated along $y$-axis in blocks 1 and 2. The cells are inflated along both $x$-axis and $y$-axis in block 3.

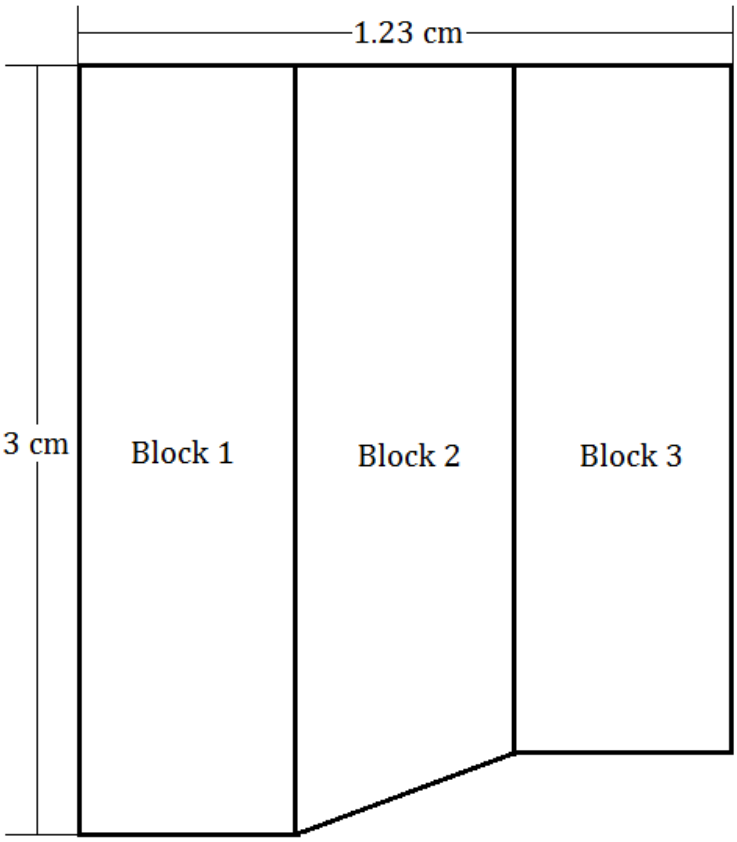


Figure 6. The configuration of flow supersonic flow over a wedge.

Only one cell is considered along $z$-axis, making the simulation 2D in $xy$-plane.

## 3.3. Initial & Boundary Conditions

The boundary conditions for various faces are described below:

a) Inlet: The left face of block 1

| | |
|---|---|
| Pressure ($p$) | 81134.8794470031 Pa |
| Temperature ($T$) | 145.768159204 K |
| Velocity vector ($\vec{u}$) | (363.02, 0, 0) m/s |

b) Outlet: The right face of block 3

| | |
|---|---|
| Pressure ($p$) | Zero Gradient |
| Temperature ($T$) | Zero Gradient |
| Velocity vector ($\vec{u}$) | Zero Gradient |

c) Bottom: The base of block 1

| | |
|---|---|
| Pressure ($p$) | Symmetry Plane |
| Temperature ($T$) | Symmetry Plane |
| Velocity vector ($\vec{u}$) | Symmetry Plane |

d) Obstacle: The base of block 2 and block 3

| | |
|---|---|
| Pressure ($p$) | Zero Gradient |
| Temperature ($T$) | Zero Gradient |
| Velocity vector ($\vec{u}$) | Slip |

e) Top: The upper face of all 3 blocks

| | |
|---|---|
| Pressure ($p$) | Zero Gradient |
| Temperature ($T$) | Zero Gradient |
| Velocity vector ($\vec{u}$) | Zero Gradient |

For initial condition, the internal field is assigned Inlet boundary condition throughout.

### 3.4. Solver

The flow through convergent-divergent nozzle governing equations, as described in section 2, are solved using rhoCentralFoam [4]. The thermophysical properties of air, assuming perfect gas, is used. The simulation type is laminar.

## 4. Results

The simulations are run on OpenFOAM 5.0 and the post processing is done using ParaView.

The pressure field and velocity magnitude at a computational time $T_{comp}$ before reaching steady state is shown in fig. 7. The bow shock is clearly visible in the contours.

As clearly indicated in the contours, there is a sudden jump in pressure across the shock while velocity drops across the shock.

Also, the shock is very well defined close to the wedge and gets smeared away from the body indicating a weak shock. This observation agrees with the discussion in section 2.1.

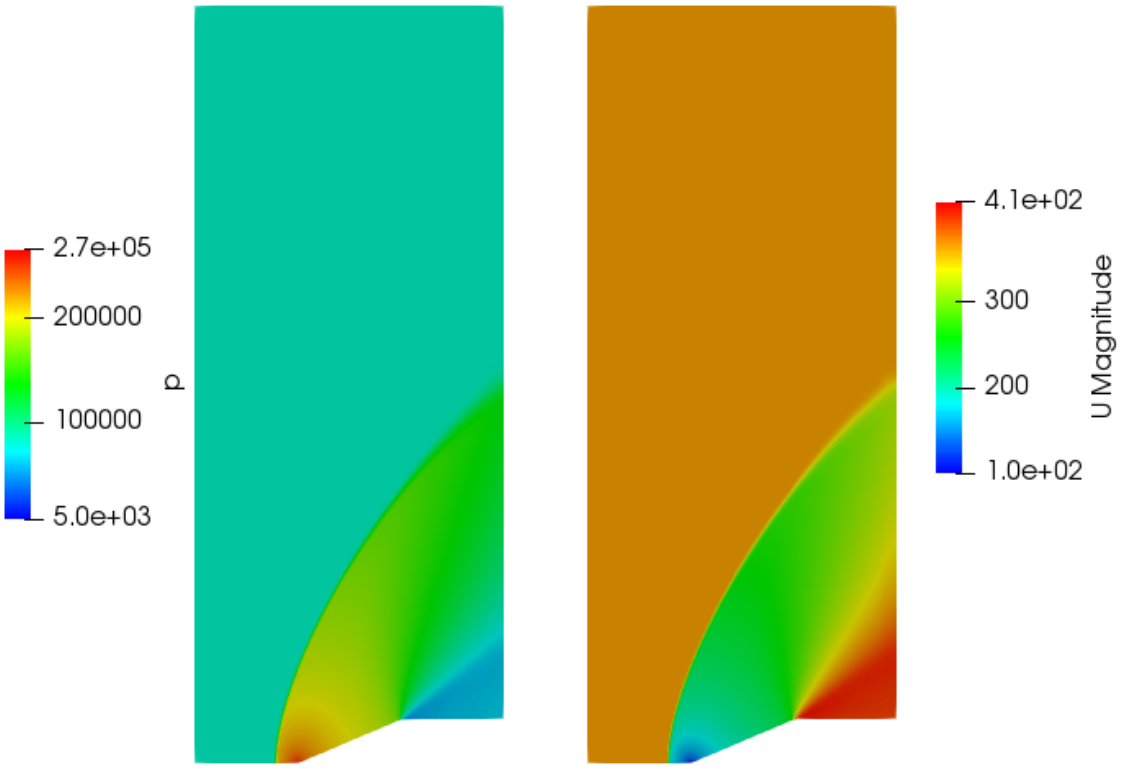


Figure 7. Pressure field and velocity magnitude at $T_{comp} = 0.00011$.

The steady-state pressure field and velocity magnitude is shown in fig. 8.

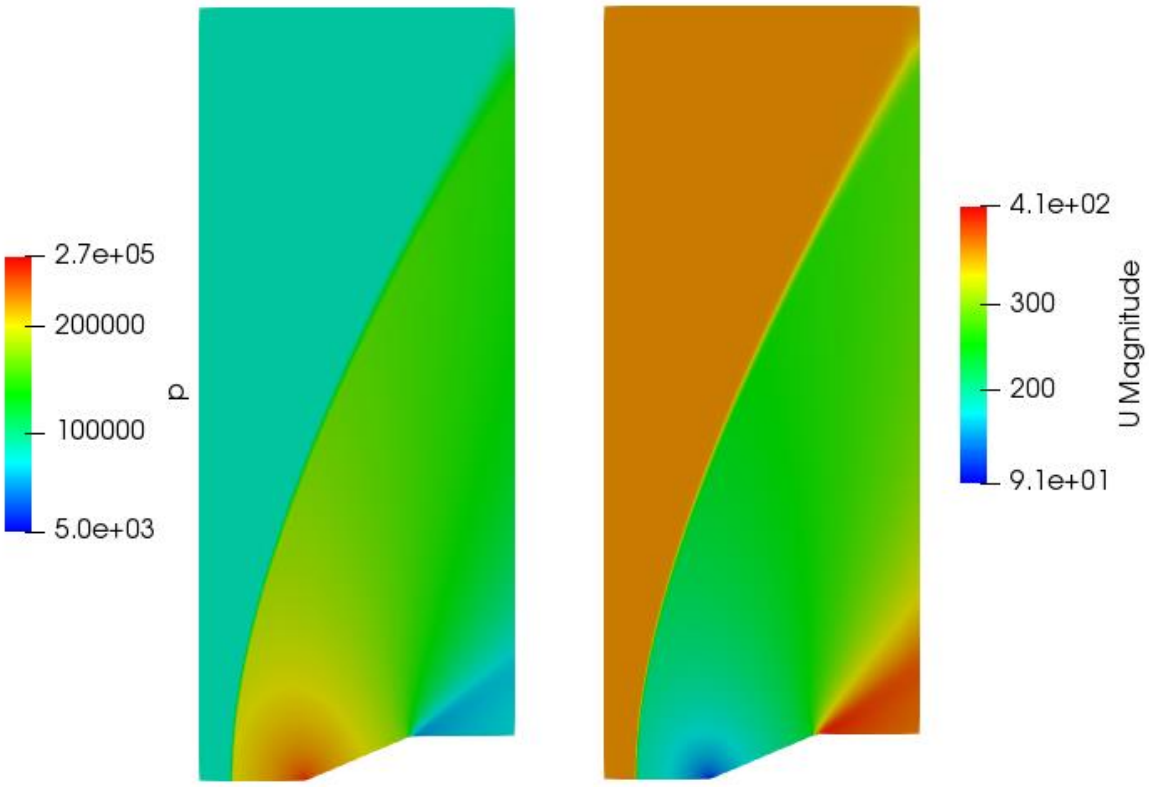


Figure 8. Steady-state pressure field and velocity magnitude.

The stand-off distance $\delta$ measured from the contour is 0.282 cm. The steady-state velocity plots along two different $y = constant$ lines are shown in fig. 9 and 10.

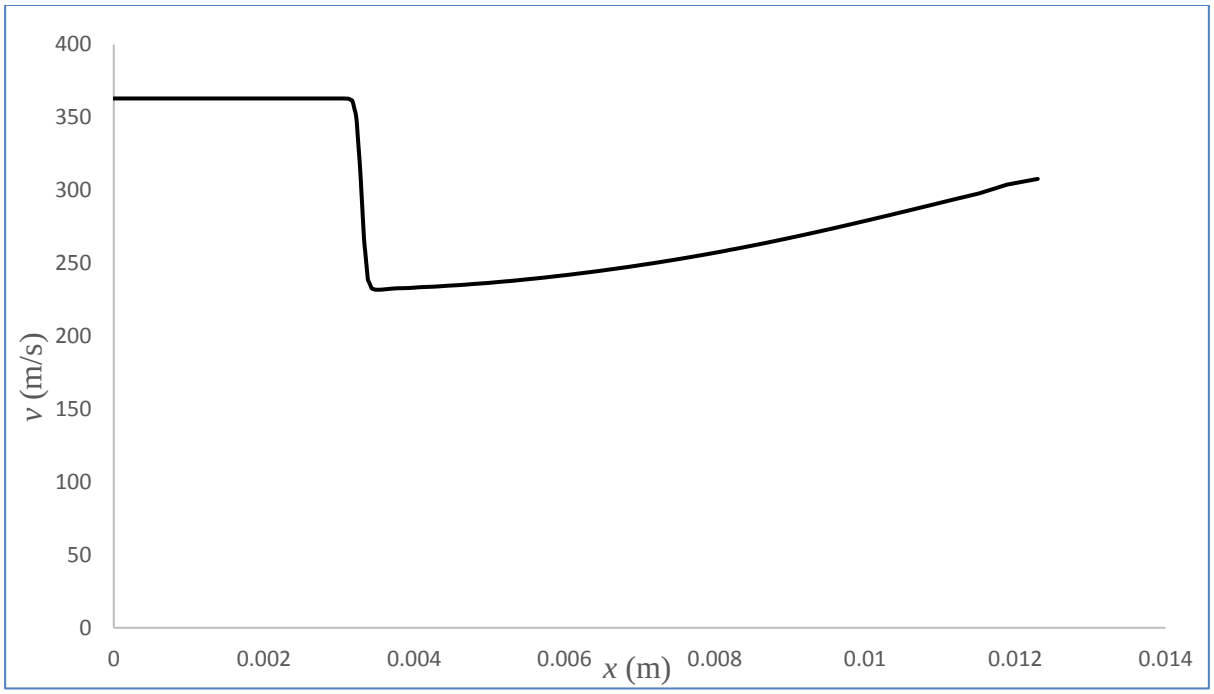


Figure 9. Variation of steady-state velocity along $x$-axis at $y = 1$ cm.

The velocity drops to 232.32 m/s across the shock at $y = 1$ cm.

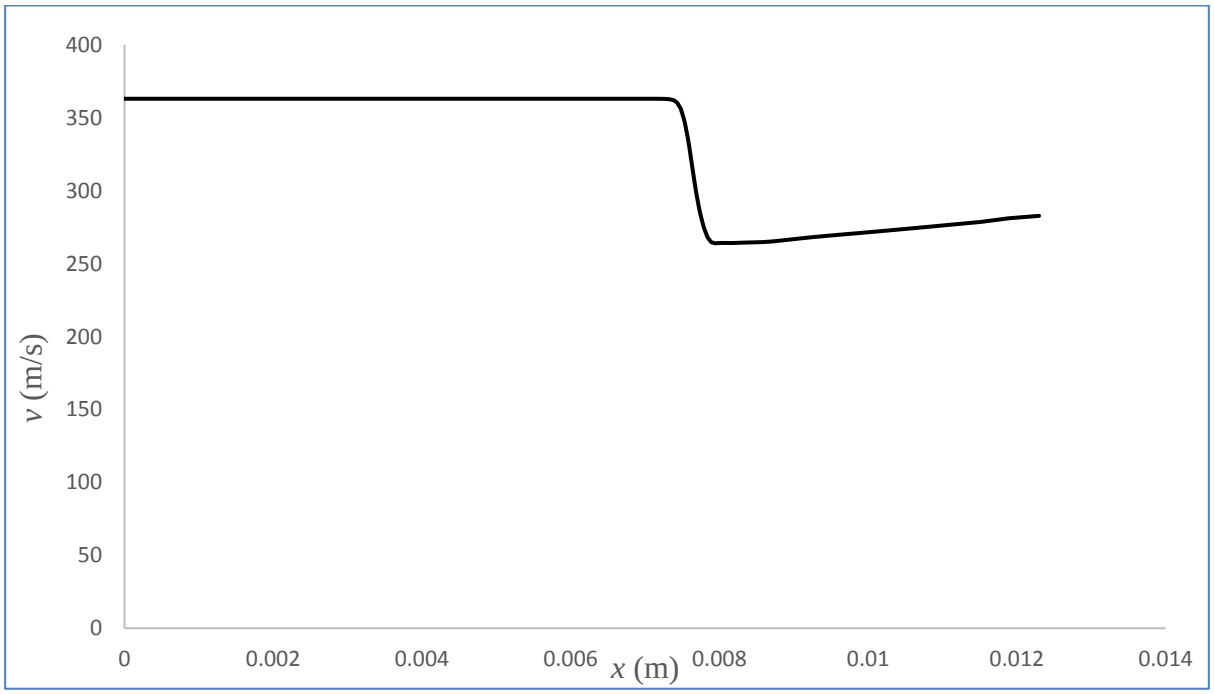


Figure 10. Variation of steady-state velocity along $x$-axis at $y = 2$ cm.

The velocity drops to 263.98 m/s across the shock at $y = 2$ cm.

The data clearly indicates that the shock at gets weaker away from the body.

The steady-state pressure plot along $y = 0$ is shown in fig. 11.

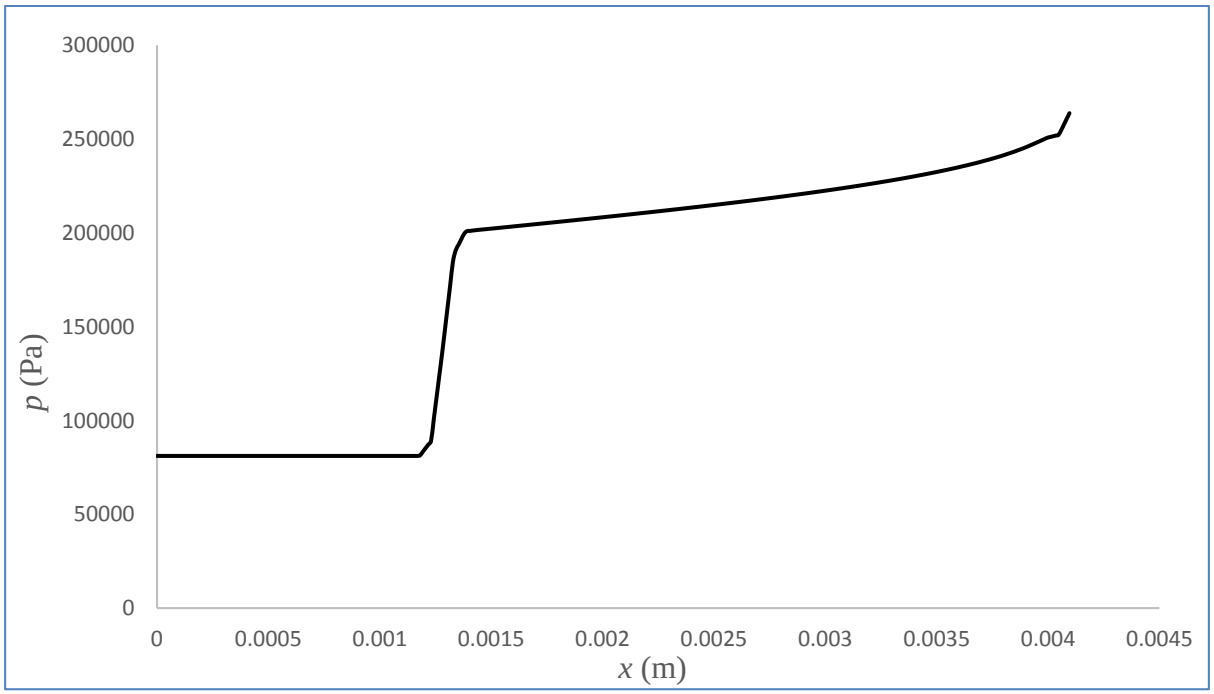


Figure 10. Variation of steady-state pressure along $x$-axis at $y = 0$.

Analysing the above data shows that the pressure ratio across the shock $p_2/p_1$ is 2.476. The normal shock relation for $M = 1.5$ shows that the pressure ratio $p_2/p_1$ is 2.458, indicating that the bow shock acts like a normal shock near the wedge, as discussed in section 2.1.

# 5. Conclusion

Supersonic flow of air over a wedge is simulated using OpenFOAM solver rhoCentralFoam. The wedge angle is more than the allowable deflection angle for the formation of an attached oblique shock for the given Mach number. The simulation produced expected result. A curved shock wave at a finite stand-off distance was produced. The pressure jump across the shock near the wedge also agreed with the normal shock relations. It was also shown that the shock waves got weaker away from the body. The simulated results match well with analytical solution.

# References


1. Anderson, J.D., Modern Compressible Flow, McGraw Hill Inc., New York, 1984.

2. Anderson, John D. Fundamentals of Aerodynamics. Boston: McGraw-Hill, 2001.

3. Liepmann, H. W. and A. Roshko, Elements of Gasdynarnics, Wiley, New York, 1957.

4. Greenshields, C. J., Weller, H. G., Gasparini, L. and Reese, J. M. (2010), Implementation of semi-discrete, non-staggered central schemes in a collocated, polyhedral, finite volume framework, for high-speed viscous flows. Int. J. Numer. Meth. Fluids, 63: 1-21. doi:10.1002/fld.2069